Figure S1. Experimental gating stratergies.

(A) All expermients were first gated on the lymphocyte population, followed by the live $CD8^+$ population, then the CD45RA/CD27 profile was obtained. Each CD45RA/CD27 defined subset was then examined for expression of γH2AX, KLRG1, CD57 and various other mitochondrial markers described in the main text. (B) Representative examples showing ROS production using MitoSox and DHE in CD45RA/CD27 $CD8^+$ T cells following overnight stimulation. P values were determined using a repeated measures ANOVA followed by the Tukey correction.

Figure S2. Cellular bioenergetic profile.

(A) Example and graph (B,C) showing CD69 expression in CD45RA/CD27 defined $CD8^+$ T cell subsets measured after overnight stimulation with 0.5μg/ml anti-CD3. Graph depicts mean ± SEM for 8 donors. (D) The XF-24 Extracellular Flux analyzer was used to perform the mitochondrial stress test, which measures several parameters of mitochondrial function in cells in real time. A typical experiment is shown here in which basal oxygen consumption rate (OCR) is allowed to stabilize before the sequential addition of oligomycin, FCCP, rotenone and antimycin A. Oligomycin, an ATP coupler which inhibits ATP synthesis by blocking complex V and is used to distinguish the percentage of oxygen consumption given over to ATP synthesis and to overcome the natural proton leak across the inner mitochondrial membrane. FCCP, uncouples ATP synthesis from the electron transport chain by transporting H^+ ions across the inner mitochondrial membrane. The collapse of the MMP leads to the consumption of both oxygen and energy without generating ATP and is used to calculate the spare respiratory capacity (SRC). Rotenone and antimycin A, block complex I and III respectively of the electron transport chain shutting down mitochondrial respiration allowing the calculation of both the mitochondrial and non-mitochondrial fractions contributing to respiration (Hill et al., 2012). This time course is annotated to show the relative contribution of non-respiratory chain oxygen consumption, ATP-linked oxygen consumption, the maximal OCR after the addition of FCCP, and the reserve capacity of the cells. (E) Graph showing the expression of Mitotracker Green on CD45RA/CD27 defined $CD8^+$ subsets following a 3 day stimulation with 0.5 μg/ml anti-CD3 and 5 ng/ml IL-2 with either 0.1% DMSO or 500 nM BIRB 796.

Graph depicts mean ± SEM for 5 donors. P values were determined using a repeated measures ANOVA followed by the Tukey correction.

Figure S3. Lack of mTORC1 activity in CD8$^+$ EMRA T cells.

(A) Time course of phospho-S6 expression in CD45RA/CD27 CD8$^+$ T cell stimulated with 0.5 μg/ml anti-CD3. Example (B) and data (C) of phospho-S6 within CD45RA/CD27 defined CD8$^+$ subsets stimulated for 2 hour stimulation with 0.5 μg/ml anti-CD3 with either 500 nM BIRB 796 (grey) or 0.1% DMSO (black). The graph shows the mean ± SEM for 5 donors. (D) Representative immunoblots and graph of CD8$^+$ T cells following siRNA knockdown of MK2, 24 and 48 hours post transduction. Example, lanes were run on the same gel but were non-contiguous, splice site represented by the black line (E) and data (F) of phopsho-S6 within stimulated CD45RA/CD27 CD8$^+$ T cells measured 48 hours following siRNA knockdown of MK2 (grey) and a control siRNA (black). The graph shows the mean ± SEM for 3 donors. All P values were determined using a repeated measures ANOVA followed by the Tukey correction.

Supplementary Figure. 1

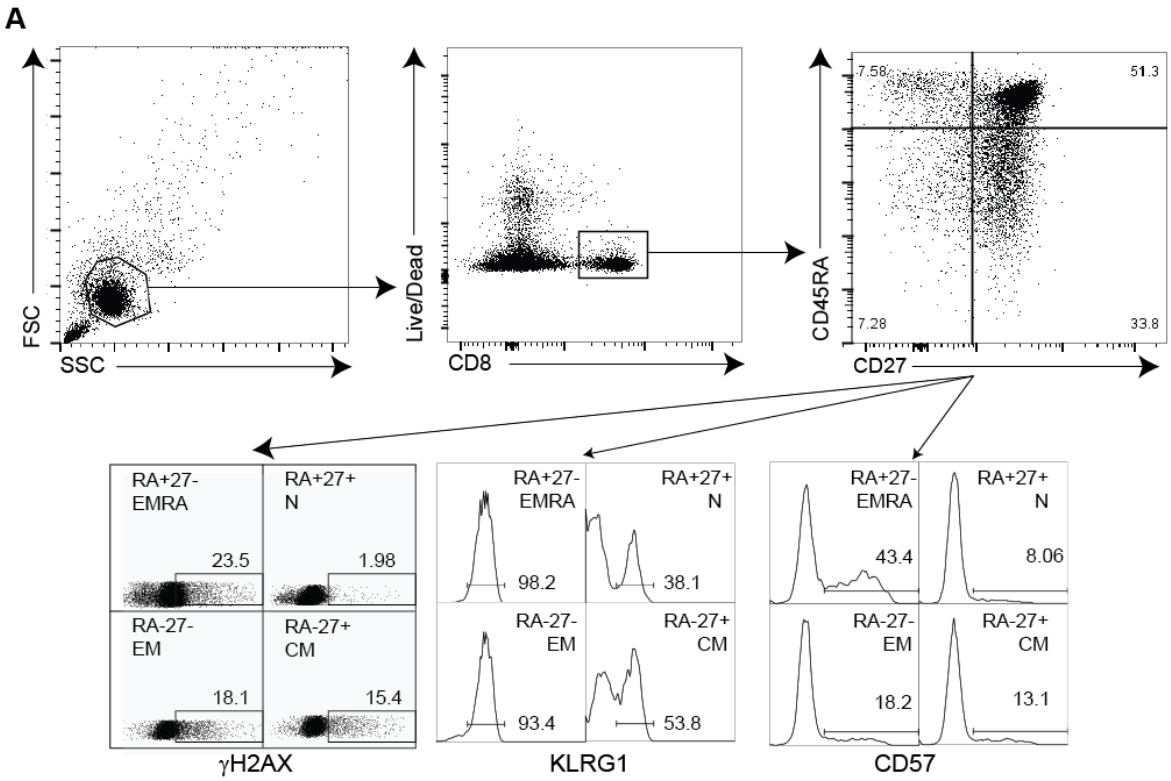

Supplementary Figure. 2

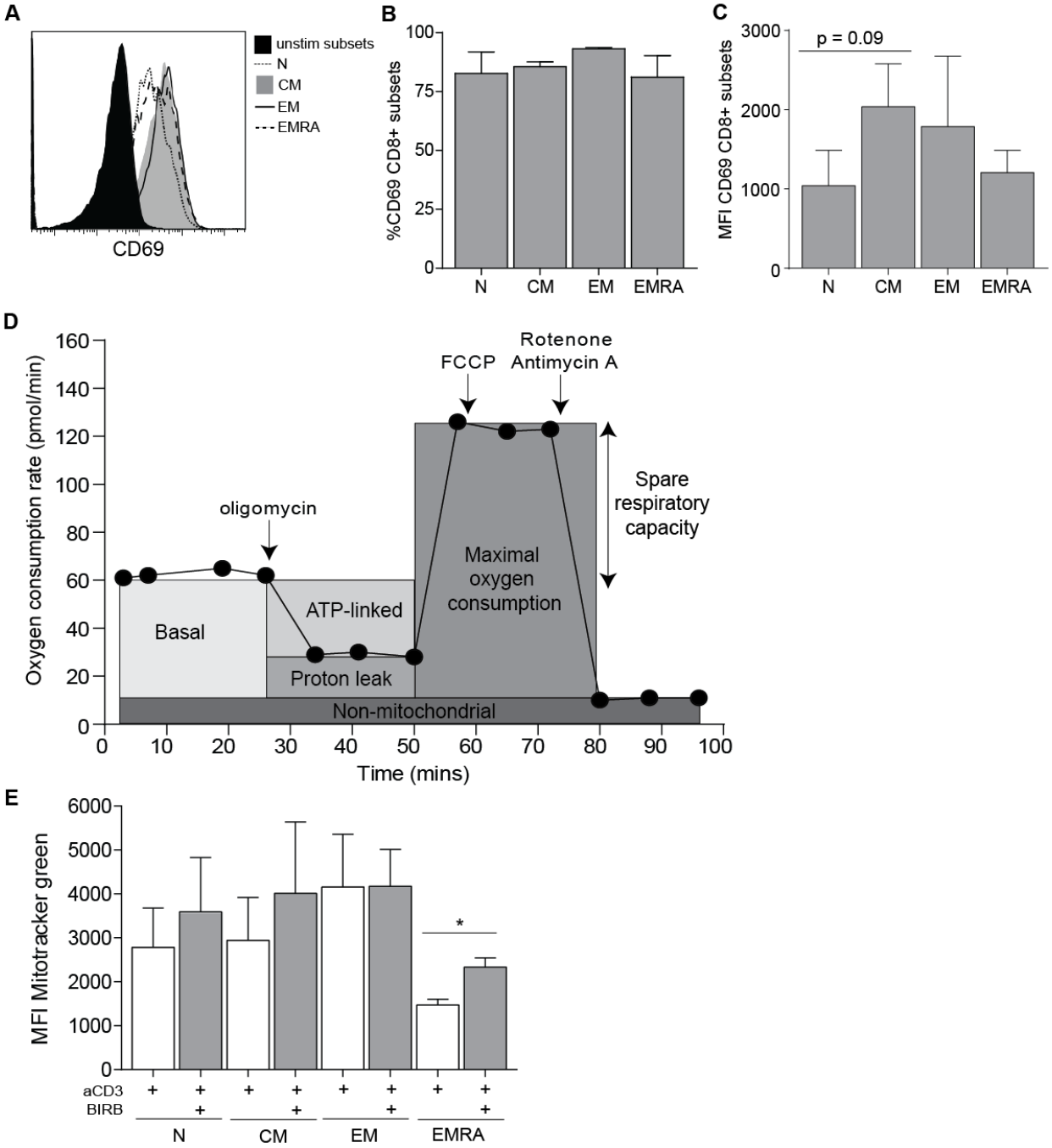

Supplementary Figure. 3